Neuro-Oncology Advances
3(1), 1–9, 2021 | doi:10.1093/noajnl/vdab019 | Advance Access date 29 January 2021

[18F]-FDHT PET/CT as a tool for imaging androgen receptor expression in high-grade glioma

Marina Orevi†, Ofer Shamni†, Nomi Zalcman†, Alexandre Chicheportiche†, Anat Mordechai†, Samuel Moscovici, Yigal Shoshan, Tal Shahar, Hanna Charbit, Mijal Gutreiman, Iddo Paldor, Eyal Mishani†, Alexander Lossos†, and Iris Lavon†

Department of Nuclear Medicine and Biophysics, Hadassah-Hebrew University Medical Center, Jerusalem, Israel (M.O., A.C.); Cyclotron/Radiochemistry Unit, Hadassah-Hebrew University Medical Center, Jerusalem, Israel (O.S., E.M.); Leslie and Michael Gaffin Center for Neuro-Oncology, Hadassah-Hebrew University Medical Center, Jerusalem, Israel (N.Z., A.M., H.C., M.G., A.L., I.L.); Agnes Ginges Center for Human Neurogenetics, Department of Neurology, Hadassah-Hebrew University Medical Center, Jerusalem, Israel (N.Z., H.C., M.G., A.L., I.L.); Department of Oncology, Hadassah-Hebrew University Medical Center, Jerusalem, Israel (A.M., A.L.); Department of Neurosurgery, Hadassah-Hebrew University Medical Center, Jerusalem, Israel (S.M., Y.S., I.P.); The Laboratory for Molecular Neuro-Oncology, Department of Neurosurgery, Shaare Zedek-Hebrew University Medical Center, Jerusalem, Israel (T.S.)

†*These authors contributed equally to the study.*

Corresponding Authors: Alexander Lossos, MD, Professor of Neurology, Head, Leslie and Michael Gaffin Center for Neuro-Oncology, Departments of Oncology and Neurology, Ein-Kerem, POB 12000, Hadassah-Hebrew University Medical Center, Jerusalem, Israel (Alos@hadassah.org.il); Iris Lavon, PhD, Head of Molecular Neuro-Oncology Lab, Neurology Department and Leslie and Michael Gaffin Center for Neuro-Oncology, Hadassah Hebrew University Medical Center, Jerusalem, Israel (IrisL@Hadassah.org.il).

Abstract

Background. G lioblastoma (GBM) is associated with poor overall survival. Recently, we showed that androgen receptor (AR) protein is overexpressed in 56% of GBM specimens and AR antagonists induced dose-dependent death in several GBM cell lines and significantly reduced tumor growth and prolonged the lifespan of mice implanted with human GBM. 16β-18F-fluoro-5α-dihydrotestosterone ([18F]-FDHT) is a positron emission tomography (PET) tracer used to detect AR expression in prostate and breast cancers. This study was aimed at exploring the ability of [18F]-FDHT-PET to detect AR expression in high-grade gliomas.

Methods. Twelve patients with suspected high-grade glioma underwent a regular workup and additional dynamic and static [18F]-FDHT-PET/CT. Visual and quantitative analyses of [18 F]-FDHT kinetics in the tumor and normal brain were performed. Mean and maximum (max) standardized uptake values (SUVs) were determined in selected volumes of interest. The patients had surgery or biopsy after PET/CT. AR protein was analyzed in the tumor samples by western blot. Fold change in AR expression was calculated by densitometry analysis. Correlation between imaging and AR protein samples was determined.

Results. In six of the 12 patients, [18 F]-FDHT uptake was significantly higher in the tumor than in the normal brain. These patients also had increased AR protein expression within the tumor. Pearson correlation coefficient analysis for the tumor-to-control normal brain uptake ratio in terms of SUV_{mean} versus AR protein expression was positive and significant (R = 0.84; $P = .002$).

Conclusion. [18 F]-FDHT-PET/CT could identify increased AR expression in high-grade glioma.

Key Points

- This study demonstrates the ability of [18F]-FDHT PET/CT to visualize AR expression in human brain tumors.
- A significant correlation (R = 0.84; $P = .002$) was shown between [18F]-FDHT uptake and AR expression.
- The results of this study pave the way for the evaluation of AR-targeted therapy in AR-expressing gliomas.

Importance of the Study

Our findings indicate that [18F]-FDHT-PET/CT holds potential as an additional tracer to detect high-grade gliomas, as well as a screening tool for non-invasive identification of androgen receptor expression and potentially might be used in the future evaluation of the therapeutic feasibility of androgen receptor antagonists in patients with glioma.

Although considerable progress has been made in understanding the molecular pathogenesis of GBM in recent times, therapeutic options and successful treatment continue to lag.[1] This era of personalized medicine obligates us to search for additional methods of diagnosis and therapies, especially for incurable, aggressive diseases with poor prognoses. From this point of view, GBM is one of the most challenging malignant forms of brain tumor, accounting for 3–4% of all cancer-related deaths.[1] It is associated with median overall survival of only 14.6 months despite the aggressive standard of care.

We have shown that AR is overexpressed in the vast majority of GBM specimens, 93% of GBM samples showed AR mRNA overexpression and 56% demonstrated high AR protein expression.[2] AR is a member of the steroid- hormone receptor superfamily, a class of receptors that function through their ability to regulate the transcription of specific genes, some of which can promote cancer cell survival and growth.[3] It is overexpressed in prostate cancer[4] and is a proven treatment target, particularly in castration resistance prostate cancer. AR is also overexpressed in 60–80% of breast cancers[5] and considered a potential therapeutic target for the triple-negative subtype.[6]

Inhibition of AR signaling *in vitro* and *in vivo* with the Food and Drug Administration (FDA) approved AR antagonists induced dose-dependent death of several GBM cell lines.[2] Furthermore, it significantly decreased the volume of human GBM implanted subcutaneous[2] in nude mice and the lifespan of the mice implanted with GBM intracranially (unpublished data). These preclinical results led us to hypothesize that anti-AR drugs could be a new potential treatment for this devastating neoplasm.

Analysis of protein expression in high-grade gliomas usually requires invasive tumor biopsy, which is not always feasible, and small stereotactic biopsy may not represent the tumor profile in its entirety. Furthermore, in GBM, necrosis may constitute over 80% of the tumor volume, leaving only a fraction of viable tumor tissue for an accurate diagnosis.[7] Also, the immunohistochemical-staining analysis relies heavily on the skill set of the trained pathologist and it is mainly qualitative. Other methods such as western blot analysis or ELISA are more quantitative methods but still require fresh or frozen tissue samples.

Non-invasive imaging tools play a very important complementary, and in the vast majority of cases, the crucial role in GBM diagnosis. While MRI is the primary clinical neuroimaging modality, molecular imaging using positron emission tomography (PET) is a well-established method in systemic oncology[8] and is being increasingly used to supplement MRI in the clinical management of brain tumors.[9,10] The ability of PET to identify biological processes occurring at the cellular and molecular levels is important in the biological characterization of the tissue of interest. Unique radiopharmaceuticals for PET/CT, such as such as [68Ga] GA-DOTA-TATE[11] [18F]-16 alpha-fluoroestradiol (-[18F]-FES),[12] and 16β-[18F]-fluoro-5α-dihydrotestosterone ([18F]-FDHT)[13] were developed for visualizing somatostatin, estrogen, and androgen receptor respectively. These tracers are used worldwide in the diagnosis, pre- and post-treatment evaluations, and patient follow-up, for neuroendocrine and prostate tumors. Imaging of metabolic processes or receptor expression, along with the unique ability of quantification, make PET/CT a very useful tool for the molecular characterization of the desired tissue of interest *in vivo*. Thus, this imaging tool has become increasingly important in providing patient-specific therapy.

After recognizing the role of the AR in GBM, we hypothesized that AR expression in GBM patients could be non-invasively evaluated using a suitable PET probe. Fluorine-18 labeled dihydrotestosterone, or [18F]-FDHT, was first described by Liu et al.[14] and has proven since to be highly accurate for detecting AR expression in prostate cancer.[15–17] A moderate correlation between [18F]-FDHT uptake and AR expression has also been shown in metastatic breast cancer lesions.[18] There is a lack of information regarding its ability to penetrate through the blood-brain barrier (BBB) of intact or in disrupted BBB, as in the case of GBM. Thus, this study aimed to examine the feasibility and accuracy of [18F]-FDHT PET/CT for detecting AR expression status in high-grade gliomas.

Methods

Study Procedure

This is a prospective two medical centers feasibility trial. The study was approved by the local ethics committee of both hospitals (HMO-611–18 and 0289-19-SZMC). Patients diagnosed by MRI with suspected high-grade glioma who were scheduled for biopsy or surgery were considered potential candidates. They had a standard workup and screening for eligibility (see below). Once participants provided written informed consent, they underwent [18F]-FDHT PET/CT, followed by surgery or biopsy, usually on the same day or one day after (Supplementary Table S1). Tissue samples were obtained from the available clinically selected site and were referred to pathology for diagnosis. A small portion of the fresh/frozen tumor specimen was analyzed for AR expression by western blot. The imaging and the molecular laboratory team were each

blinded to the other group's results. Finally, the AR protein and mRNA expression in the tumor was compared to [18F]-FDHT accumulation in the tumor, which was analyzed semi-quantitatively by determining the standardized uptake value SUV_{max} and SUV_{mean} tumor-to-normal brain ratios. Correlation between the results of the AR protein and mRNA expression in the tumor and the quantitative results of [18F]-FDHT PET/CT was calculated.

Patients

Patient characteristics are summarized in Table 1 and Supplementary Table S1. From January 2019 to March 2020, 12 patients, ie, six men and six women age ranging between 31–86 years (age mean: 62.75 years) were included according to the following criteria; suspicion of high-grade glioma, age above 18 years, signed informed consent, Karnofsky Functional Scale of ≥70, planned surgery/biopsy and physical ability to lie down calmly for an hour. Exclusion criteria were as follows: the presence of prostate cancer, exceptional laboratory values (bilirubin level: >1.5 × ULN, AST/ALT level: >2.5 × ULN, albumin level: <2 g/dl, creatinine level: >2.5 mg/dl, and calcium level >11 mg/dl), presence of other diseases in which PET/CT and MRI are contraindicated, and claustrophobia.

Tumor location included the left frontal lobe (n = 4); the right temporal lobe (n = 2); and one lesion in each the left temporal, left occipito-parietal, left parietal, left temporo-parieto-occipital-corpus callosum, bilateral gliomatosis, and mid-frontal-corpus callosum. All patients except patient #5 were naïve to treatment before the PET or surgery (Supplementary Table S1). Ten patients were referred from the emergency room, one from the neurology department, and one from the neurosurgery department. Most patients (11/12) had no history of cancer. One patient (#12) had colon cancer, melanoma in situ, and basal cell carcinoma with complete remission for 6, 8, and 19 years, respectively, before the diagnosis of GBM. Most patients had a Karnofsky score of 80, one patient (#5) had a score of 90, and one (#1) had a score of 70 (mean score: 80). Four of the 11 patients with gliomas were treated with dexamethasone (4–12 mg/day).

Radiochemical Synthesis of [18F]-FDHT

[18F]-FDHT was synthesized as previously described[19] with minor modifications, using a Synthra RNplus module (Synthra GMBH, Hamburg, Germany) in a fully automated process with an overall radiosynthesis time of 100 min, the radiochemical yield of 16.43 ± 2.6% (n = 10), decay corrected to the end of the bombardment, and radiochemical purity routinely greater than 99%. Quality control was performed by radio-TLC and analytical reverse-phase HPLC, by using co-elution with a non-radioactive reference standard, FDHT (ABX, Radeberg, Germany). Additional QC included the confirmation of a clear appearance and colorlessness, radioactive half-life, radionuclide identity, pH, residual solvents by gas chromatography, colorimetric determination of Kryptofix content, sterility, apyrogenicity, and filter integrity. All QC results were under previously published specifications. The final product was formulated in <9% ethanol in sterile saline solution and was further diluted with sterile saline solution before being dispensed in sterile vials in a class A radiopharmaceutical dispensing unit.

[18F]-FDHT PET/CT Data Acquisition and Image Reconstruction

All scans were performed using a GE Healthcare (Milwaukee WI, USA) Discovery MI digital PET/CT system. The scanner combines a 128-slice CT system and a 4-ring PET system with LightBurst digital detectors providing a 20 cm axial field-of-view and a 70 cm transaxial field-of-view. The system is the time of flight (TOF)-capable with a timing resolution of about 380 ps.[20]

Patients underwent dynamic [18F]-FDHT brain PET followed by static whole-body acquisition as part of the research protocol. Dynamic PET studies were started immediately with the intravenous injection of 315.2 ± 39.9 MBq (range: 240.0–384.0 MBq) [18F]-FDHT. Scans were acquired as a series of 14 frames for a total duration of 30 min (10 frames of 1 min followed by four frames of 5 min). The static PET acquisitions started at a mean of 67 ± 6 min (range, 57–77 min) after tracer injection and were performed from the proximal femur to the base of the skull with an acquisition time of 2.0 min per bed position. Dynamic and static studies were reconstructed using the GE VUE Point FX-S (VPFX-S) algorithm, a 3D maximum likelihood ordered subset expectation maximization (3D OSEM) image reconstruction algorithm with three iterations, eight subsets, and 6-mm post-processing filter and by using TOF information and point spread function modeling. All data were corrected from scattering, random events, and dead time. A CT scan was acquired before each PET study for attenuation correction.

Image Analysis

Visual estimation of the images at all phases was performed by an experienced dual-trained radiologist/nuclear medicine specialist who had access to the medical history and imaging data but not to the pathology or AR analysis data. [18F]-FDHT uptake intensity higher than that in normal brain tissue was considered positive, and uptake intensity equal to or lower than that in the normal brain was considered negative.

In addition to visual evaluation, all PET images were analyzed quantitatively using the Inveon Research Workplace (IRW) 4.1 Software (Siemens Preclinical Solutions, Knoxville Tennessee, USA). To estimate the tracer uptake in GBM and to compare it with AR protein expression collected (after biopsy or surgery) few days after the PET examination, volumes of interest (VOIs) were located around the biopsy site or over the surgery area on PET images and SUV_{max} and SUV_{mean} values were measured in these VOIs. For this purpose, dynamic and static PET studies were co-registered with post-op CT or MRI, allowing for delineation and transfer of the biopsy or surgery area VOIs from CT or MRI to the PET studies.

Table 1. Patient parameters and AR expression measured from tissue samples and $SUV_{mean/max}$/Control values obtained from [18F]-FDHT PET/CT scans from the 12 patients included in this study. Pearson's r correlation coefficients and *P* values are also presented

Patient	Age	Sex	Pathology	Location	KPS	AR protein tumor/ NB	SUV_{mean}/ Con	SUV_{max}/ Con
1	79	M	Glioblastoma, IDH Wild type	Mid-frontal/corpus callosum	70	1.3	0.6	0.7
2	62	M	Glioblastoma, IDH Wild type	Right temporal	80	2.2	1.5	1.6
3	53	F	Anaplastic Astrocytoma, IDH Mutant	Bilateral gliomatosis	80	Un-available	0.96	0.91
4	63	M	Glioblastoma, IDH Wild type	Right temporal	80	1.9	1.5	1.7
5	31	F	Glioblastoma, IDH Wild type	Left occipito-parietal	90	2.3	2.5	3.4
6	54	M	Glioblastoma, IDH Wild type	Left frontal	80	2.8	2.6	2
7	69	F	Glioblastoma, IDH Wild type	Right temporo-parieto-occipital corpus callosum	80	1.9	1.6	1.7
8	39	M	Oligodendroglioma, IDH Mutant	Left frontal	80	1.1	0.6	1.0
9	72	F	Anaplastic Astrocytoma, NOS	Left frontal	80	3.1	1.8	2.1
10	86	F	Glioblastoma, IDH Wild type	Left parietal	80	1.5	1.3	1.3
11*	76	M	Demyelination disease	-	80	1.1	0.82	0.6
12	69	F	Glioblastoma, IDH Wild type	Left temporal	80	0.8	0.68	1.00
r score AR protein expression SUV/Con							*0.84*	*0.67*
P value							*.002*	*.03*

* non tumoral lesion; NB, normal brain.

IRW proposed two types of automatic or manual registration [Inveon TM Research Workplace 4.1 User Manual. Siemens Preclinical Solutions; 2012]. Rigid registration involves translation and rotation of the target (PET) dataset to match the source (CT or MRI). Affine registration is a more advanced image registration algorithm that also involves scaling and shearing. An additional option allowed landmark registration on corresponding points to guide the registration algorithms. In all cases, registration between dynamic or static PET and post-op CT or MRI was first performed using automatic rigid registration followed by adjustment using the manual rigid registration tool. VOI creation included either semi-automatic (threshold approach) or manual three-dimensional delineation on anatomical (CT or MRI) or functional (PET) images. As a control, one spherical VOI in each brain hemisphere was drawn on the tumor surrounding normal brain tissues. After transferring different VOIs (for tumor and control) from anatomical images (MRI or CT) to dynamic and static PET, SUV_{max} and SUV_{mean} data were collected and decay-corrected. Time activity curves showing the tracer kinetics in the tumor and control areas were built, and the SUVtumor/control ratio obtained from late static PET scans were calculated for comparison and correlation with AR protein expression data.

Handling and Measurement of AR Expression

The tumor specimens collected following the PET scan were frozen in liquid nitrogen until RNA and protein isolation and centrally analyzed at the molecular neuro-oncology lab.

Western blot analysis

Western blotting was performed as previously described[2] with minor modifications. Briefly, tissue samples were homogenized in 200 µL of Lysis Buffer 6# (catalog no:895561, R&D Systems, Minneapolis, Minnesota, USA) supplemented with protease inhibitors (Thermo Fisher Scientific Inc Waltham, Massachusetts, USA). Protein was extracted according to the manufacturer's instructions. Tissue lysates containing 50 µg of protein were separated on 4–20% Tris-Glycine SDS-PAGE gel (Bio-Rad, Hercules, CA, USA) and assessed according to western blot analysis, along with sequential probing with an antibody against AR (D6F11 XP® Rabbit mAb 1:1000 dilution Cell Signaling Technology, Danvers, MA, USA) and GAPDH (D4C6R Mouse mAb diluted 1:1000, Cell Signaling Technology), with the relevant secondary horseradish peroxidase-conjugated antibody (Santa Cruz Biotechnologies, Dallas, Texas, USA).

Blots were quantified using ImageJ software,[21] following normalization to GAPDH expression levels.

RNA Extraction, cDNA Preparation, and qPCR

Total RNA was isolated from snap-frozen gliomas with TRI Reagent® (Sigma-Aldrich, Rehovot, Israel), according to the manufacturer's instructions. Control RNAs were obtained from a commercial mix pooled from 23 donors (mean age, 68 years; 13 men and 10 women) (FirstChoice® Human Brain Reference Total RNA, Thermo Fisher Scientific Inc., Waltham, MA, USA).

cDNA was produced from 0.2 ug total RNA with a qScript cDNA Synthesis Kit (Quanta Biosciences, Gaithersburg, MD, USA), according to the manufacturer's instructions.

Real-time PCR amplification and relative quantification were analyzed with StepOne real-time RT PCR (Life Technologies). The reaction mix included 1 μl cDNA, and 300 nmol/l of each of the primers indicated below (Syntezza, Jerusalem, Israel): and 5 μl of SYBR green mix (Perfecta Syber Green Fast Mix ROX, Quanta Biosciences) in a total 10 μl volume. The fold changes of the target mRNAs were normalized to HPRT and TBP1. Then the fold changes of each mRNA were calculated based on the ratio between the tumor sample and the normal brain. The experiment was repeated three times in triplicate. The results are presented as the relative quantification compared to the normal brain.

AR(1)-F:ACCGAGGAGCTTTCCAGAATC,
AR(1)-R:AGGCTCTGGGACGCAACCT;
HPRT-F:GATGGTCAAGGTCGCAAGC,
HPRT-R:ATATCCTACAACAAACTTGTCT GGAA;
TBP-1-F:CCACTCACAGACTCTCACAAC,
TBP-1-R:CTGCGGTACAATCCCAGAACT

Statistical Analysis

AR protein and mRNA expression were correlated to each other and [18F]-FDHT PET/CT findings within the tumor. Correlations between mRNA relative quantification or semi-quantitative androgen receptor protein analysis within the tumor and [18F]-FDHT uptake (SUV_{max} and SUV_{mean}) were quantified using the Pearson correlation coefficient *r*. A *P* value of 0.05 or less was considered significant.

Results

Patients

Eleven out of 12 patients completed the dynamic and static phases of [18F]-FDHT PET/CT without showing adverse reactions or any complications. Patient #4 asked to stop the dynamic scan in the tenth minute and was able to resume only the late static phase. The vast majority of the participants underwent surgery/biopsy the day after PET/CT (the median interval between PET/CT and biopsy/surgery = 1). The surgery of patient #5 was performed 444 days before the PET and his inclusion was based on the results of the previous biopsy. Patient 11 was recruited due to the impression that his brain lesion was compatible with GBM, but the pathological evaluation showed a demyelination disease (Supplementary Table S1).

[18F]-FDHT PET/CT

Visual evaluation of the scans revealed five cases (patients 2, 4–7) with clear findings and very good target-to-background ratios that allowed simple recognition of increased [18F]-FDHT accumulation in the brain tumors. In an additional five cases (patients 1, 8–10, 12), visualization was quite good but with a less sharp target-to-background relationship. In two cases (patients 3 and 11), no increased uptake was noticed visually. In the first case, patient number 3, the absence of increased focal accumulation of [18F]-FDHT correlated with diffuse brain involvement by gliomatosis cerebri. Patient number 11, however, was included due to MRI findings suggesting GBM but was finally diagnosed with a plaque as part of the demyelination process (examples in Figure 1).

Dynamic Scans and Time-Activity Curves

Quantitative analysis of [18F]-FDHT kinetics in the brain tumor and normal brain was performed as described earlier by defining a VOI at the site of the tumor biopsy and two spherical VOIs as controls from normal-looking brain ipsi- and contralateral hemispheres to the tumor side. In all cases, quick initial wash-in was visualized in tumors and normal brain areas, reaching the maximum uptake at a range of 0.5–3.5 min (mean: 2.8 min) and 0.5–4.5 min (mean: 2.5 min) post-injection, respectively (examples at Figure 1 A, B). Washout was noticed in all the areas as a relative $SUV_{max/mean}$ plateau at approximately 15–30 min after injection (mean: 20 min). No consistent changes in the intensity of [18F]-FDHT accumulation were noticed between the 30 min scan at the end of the dynamic phase and the 60 min static imaging. The intensity of [18F]-FDHT uptake in the tumor at 60 min after injection ranged from SUV_{max} 0.45 to 2.30, with a mean value of 0.96 ± 0.56. The same area showed a SUV_{mean} range of 0.17 up to 0.96, with a mean value of 0.52 ± 0.24. The ratio of [18F]-FDHT accumulation in the tumor to the mean accumulation in normal brain in the ipsi and contralateral hemispheres at 60 min ranged from (SUV/Control) 0.2 to 3.4 for SUV_{max} and 0.6 to 2.6 for SUV_{mean}. No significant difference was noticed between normal brain uptake ipsi- and contralateral to the tumor (Δ_{max} range: 0.01–0.67; Δ_{mean} range: 0.03–0.83). No significant correlation (Pearson's $r = 0.2$ with $P = .5$) was noticed between the grade of tumor and intensity of uptake or the tumor-to-normal brain ratio.

AR expression in the tumor

Western blot was performed to examine AR protein expression in 11/12 lesions (the lesion of patient #3 was unavailable). The pathological analysis revealed that ten lesions were compatible with gliomas and one showed

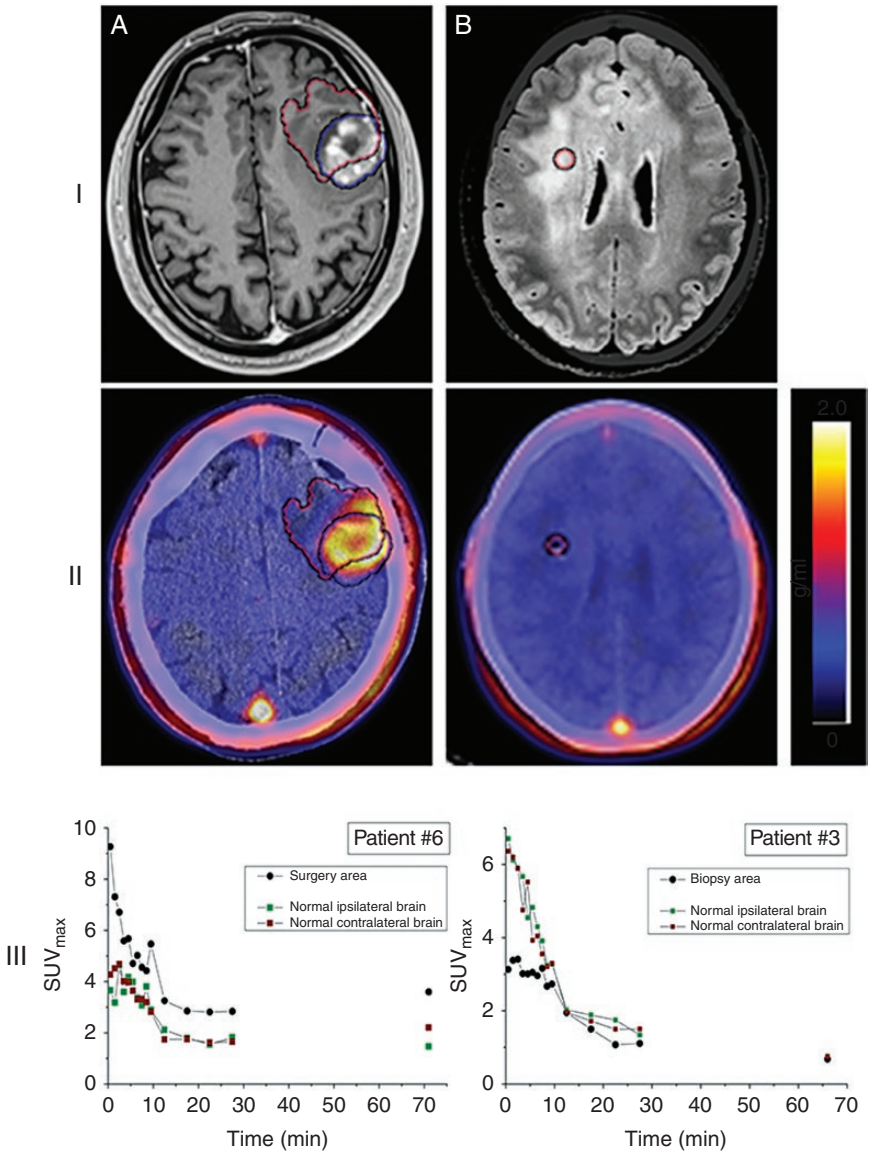

Figure 1. [18F]-FDHT uptake in high-grade gliomas. (I) MRI and (II) PET (registered with post-op CT/MRI) transaxial slices showing (A) high (patient #6), and (B) no (patient #3, gliomatosis cerebri) [18F]-FDHT uptake on static PET images acquired about 60 min after radiopharmaceutical injection. Blue and red VOIs represent respectively the tumor and biopsy/surgery area on MRI and PET slices. (III) Time-activity curves in terms of SUVmax corresponding to the biopsy/surgery area and normal ipsi- and contralateral brain. The color scale next to each PET image represents the SUV in units of g/mL.

demyelination disease. Sixty percent (6/10) of the gliomas demonstrated high expression of the AR protein (>1.9-fold) (Figure 2).

Concordance between [18F]-FDHT uptake and AR protein expression in the tumor

The correlation between [18F]-FDHT uptake and semi-quantitative AR expression and was calculated using Pearson's r correlation coefficient. At ~60 min after injection, five of the 12 patients showed significantly higher tumor accumulation of [18F]-FDHT compared to normal brain (SUVmean/control: 1.5- to 2.6-fold; SUVmax/control: 1.6- to 3.4-fold) (marked in red in Table 1). Subset with higher [18F]-FDHT tumor uptake also showed high AR protein expression within the tumor, in comparison to the AR protein expression in normal brain tissue (1.9- to 3.1-fold). Pearson correlation coefficient analysis for the (SUV/control) mean at ~60 min after the injection versus AR protein expression showed a high and significant correlation ($r = 0.84$; $P < .002$) (Table 1; Figure 3).

Calculation of Pearson's correlation coefficient showed a linear relationship between [18F]-FDHT accumulation and AR expression, from 0.67 up to 0.084. The P-value for the

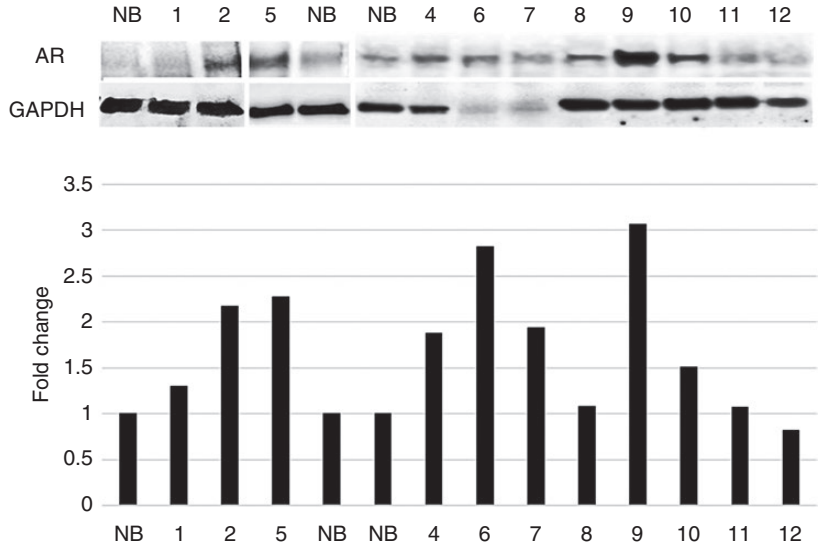

Figure 2. AR expression in tumor tissue samples. Western blot analysis by sequential probing with an antibody against AR or GAPDH in high-grade glioma samples and normal brain (NB). The western blot figure is composed of three gels. Protein fold change (Y-axis) of each tumor sample compared with that of NB was calculated using band densitometry analysis with ImageJ software, after normalization to GAPDH (lower panel).

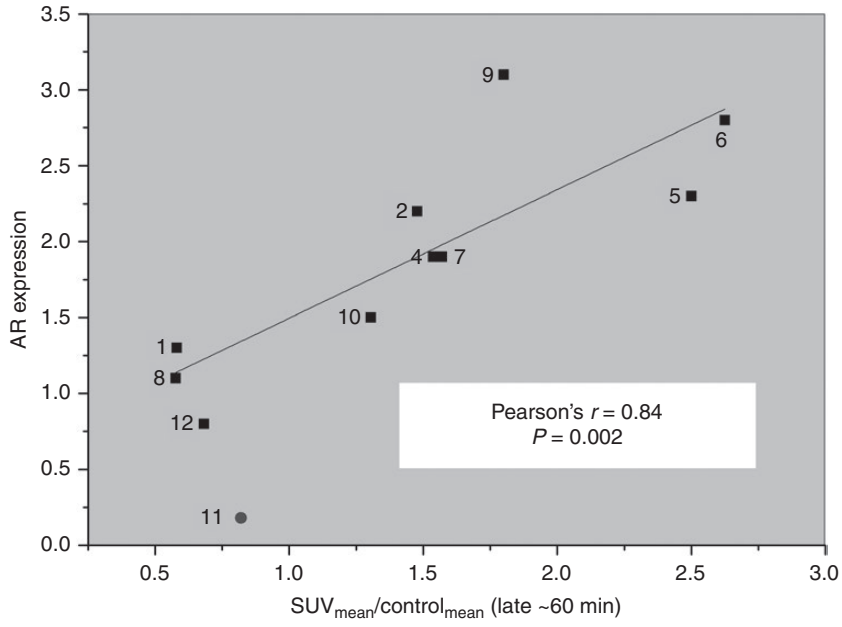

Figure 3. Correlation plot - AR expression Vs. [18F]-FDHT uptake. AR expression measured in tumor tissue samples obtained against the SUV_{mean}/$Control_{mean}$ ratio determined using [18F]-FDHT imaging done on 10/12 patients (the lesion of patient #3 was unavailable and the pathological analysis of patient #11 revealed demyelination disease-and thus wasn't included in the correlation analysis - marked in red). Pearson's correlation coefficient r and *P*-value are also presented.

correlation ranging from 0.002 to 0.03. There is no correlation between $SUV_{max/mean}$ and WHO grade or $SUV_{max/mean}$ and IDH.

There was no correlation between AR mRNA and AR protein expression (r = 0.29; *P* = .34) (Supplementary Figure S1), and between AR mRNA expression and accumulation of [18F]-FDHT within the tumor (r = 0.03; *P* = .94). All patients underwent their therapy according to plan and showed acceptable management.

Discussion

This is the first study that demonstrates the ability of [18F]-FDHT PET to detect AR expression in human brain tumors. We identified low uptake of [18F]-FDHT in the normal human brain. However, there was a significantly higher tracer accumulation (1.5–2.6-fold SUV_{mean}/normal) in 60% of the glial tumors. These tumors also had an increased AR protein expression measured by western blot analysis in the fresh/frozen tumor tissue (1.9- to 3.1-fold). This finding is in concordance with our previous study which detected high expression of AR protein expression in 56% of GBMs.[2] Pearson correlation coefficient analysis for the (SUV_{mean}/Control) at ~60 min after the injection versus AR protein expression showed a positive and significant correlation ($R = 0.84$; $P = .002$).

No correlation was evident between AR mRNA and AR protein expression. This is in concordance with the result of our previous study.[2]

Among the variety of imaging agents that have been already investigated and are still under research for brain tumor assessment, [18F]-FDHT is new in this field. Because about 50%–60% of the high-grade gliomas express the high level of AR protein, the ability of [18F]-FDHT PET/CT to demonstrate AR in these tumors non-invasively, provides a new tool for further tumor characterization and establishes a new biomarker.

In the era of precision medicine and tailored individualized therapies, our results indicate that [18F]-FDHT holds potential for differentiating AR-positive from AR-negative GBM, and therefore may provide stratification patients before treatment with AR antagonists.

Although the intensity of [18F]-FDHT uptake in our small patient cohort was relatively low (especially in comparison to fludeoxyglucose (FDG) or receptor-binding tracers like somatostatin based or prostate-specific membrane antigen (PSMA)), the high target-to-background ratio and the standard visual estimation with a simple threshold based on the premise that any uptake above the background should be considered abnormal, yielded reliable results, interpreting these studies simple. A similar approach based on a high target-to-background ratio offers a major advantage over the widely used FDG, whose major limitation is high physiological brain uptake. Thus, for example, PSMA as a biomarker of angiogenesis shows increased uptake in the endothelium of tumor but shows low expression in normal vasculature or cancer cells as well as in normal brain tissue.[22,23] Mahzouni et al. showed that two-thirds of GBMs highly expressed PSMA uptake in their neovasculature.[24] Therefore, peptide therapy with α/β-emitters based on [68Ga]Ga-PSMA PET/CT is under consideration and investigation.[25]

Production of [18F]-FDHT and scan acquisition is quite easy, and the tracer is metabolically stable and was found among several fluorinated AR ligands with the highest AR and SHBG as well as lowest progesterone receptor affinity.[15]

Despite the small number of participants, the study results demonstrated a very strong correlation between imaging and the fresh tissue results that were significant enough for the primary endpoint.

We did not analyze the levels of circulating testosterone in peripheral blood because a previous study reported no correlation between [18F]-FDHT tumor uptake and levels of testosterone.[18]

AR-targeted therapy has not yet been studied in GBM patients, but the results of our preclinical trials present the promising basis for the future.[2] Considering the preclinical results and the results obtained in other AR-positive tumors, clinical studies exploring the efficacy of AR-targeted therapy in AR-positive gliomas will be of great interest.

Identification of AR-expressing gliomas using PET scan may allow selection of patients who are candidates for treatment using androgen receptor antagonists and will enable monitoring of the expression status of the androgen receptors during the treatment.

Conclusion

The findings indicate that [18F]-FDHT PET/CT can be used as a screening tool for noninvasive identification of AR in GBM and can be useful for further evaluation of therapeutic feasibility of AR antagonists in glioma therapy.

Supplementary material

Supplementary material is available at *Neuro-Oncology Advances* online.

Keywords

androgen receptor | [18F]-FDHT | high-grade gliomas | PET/CT

Funding

We are grateful for support from Gessner Fund for Medical Research, The Samuel S. Feibus Endowment for brain tumor research, and for the generous donation of Leslie and Michael Gaffin.

Conflict of interest statement. All authors disclosed no financial relationships relevant to this publication.

Authorship Statement. Generated hypotheses, designed experiments, interpreted data, and wrote the manuscript: M.O., I.L., A.C., O.S., E.M., N.Z., A.M. Performed experimental procedures: M.O., A.C., O.S., N.Z., H.C., M.G., S.M., Y.S., I.P., T.S. Study coordinator: A.M.

References

1. Lukas RV, Wainwright DA, Ladomersky E, Sachdev S, Sonabend AM, Stupp R. Newly diagnosed glioblastoma: a review on clinical management. *Oncology (williston park).* 2019;33(3):91–100.
2. Zalcman N, Canello T, Ovadia H, et al. Androgen receptor: a potential therapeutic target for glioblastoma. *Oncotarget.* 2018;9(28):19980–19993.
3. Tan MH, Li J, Xu HE, Melcher K, Yong EL. Androgen receptor: structure, role in prostate cancer and drug discovery. *Acta Pharmacol Sin.* 2015;36(1):3–23.
4. Fujita K, Nonomura N. Role of androgen receptor in prostate cancer: a review. *World J Mens Health.* 2019;37(3):288–295.
5. Kono M, Fujii T, Lim B, Karuturi MS, Tripathy D, Ueno NT. Androgen receptor function and androgen receptor-targeted therapies in breast cancer: a review. *JAMA Oncol.* 2017;3(9):1266–1273.
6. Gerratana L, Basile D, Buono G, et al. Androgen receptor in triple negative breast cancer: a potential target for the targetless subtype. *Cancer Treat Rev.* 2018;68:102–110.
7. Kleihues P, Sobin LH. World Health Organization classification of tumors. *Cancer.* 2000;88(12):2887.
8. Boellaard R, Delgado-Bolton R, Oyen WJ, et al.; European Association of Nuclear Medicine (EANM). FDG PET/CT: EANM procedure guidelines for tumour imaging: version 2.0. *Eur J Nucl Med Mol Imaging.* 2015;42(2):328–354.
9. Albert NL, Weller M, Suchorska B, et al. Response assessment in neuro-oncology working group and European association for neuro-oncology recommendations for the clinical use of PET imaging in gliomas. *Neuro Oncol.* 2016;18(9):1199–1208.
10. Langen KJ, Galldiks N, Hattingen E, Shah NJ. Advances in neuro-oncology imaging. *Nat Rev Neurol.* 2017;13(5):279–289.
11. Moradi F, Jamali M, Barkhodari A, et al. Spectrum of 68Ga-DOTA TATE uptake in patients with neuroendocrine tumors. *Clin Nucl Med.* 2016;41(6):e281–e287.
12. Kiesewetter DO, Kilbourn MR, Landvatter SW, Heiman DF, Katzenellenbogen JA, Welch MJ. Preparation of four fluorine- 18-labeled estrogens and their selective uptakes in target tissues of immature rats. *J Nucl Med.* 1984;25(11):1212–1221.
13. Brandes SJ, Katzenellenbogen JA. Fundamental considerations in the design of fluorine-18 labeled progestins and androgens as imaging agents for receptor-positive tumors of the breast and prostate. *Int J Rad Appl Instrum B.* 1988;15(1):53–67.
14. Liu A, Dence CS, Welch MJ, Katzenellenbogen JA. Fluorine-18-labeled androgens: radiochemical synthesis and tissue distribution studies on six fluorine-substituted androgens, potential imaging agents for prostatic cancer. *J Nucl Med.* 1992;33(5):724–734.
15. Bonasera TA, O'Neil JP, Xu M, et al. Preclinical evaluation of fluorine-18-labeled androgen receptor ligands in baboons. *J Nucl Med.* 1996;37(6):1009–1015.
16. Larson SM, Morris M, Gunther I, et al. Tumor localization of 16beta-18F-fluoro-5alpha-dihydrotestosterone versus 18F-FDG in patients with progressive, metastatic prostate cancer. *J Nucl Med.* 2004;45(3):366–373.
17. Dehdashti F, Picus J, Michalski JM, et al. Positron tomographic assessment of androgen receptors in prostatic carcinoma. *Eur J Nucl Med Mol Imaging.* 2005;32(3):344–350.
18. Venema CM, Mammatas LH, Schröder CP, et al. Androgen and estrogen receptor imaging in metastatic breast cancer patients as a surrogate for tissue biopsies. *J Nucl Med.* 2017;58(12):1906–1912.
19. Ackermann U, Lewis JS, Young K, et al. Fully automated synthesis of [(18) F]fluoro-dihydrotestosterone ([(18) F]FDHT) using the FlexLab module. *J Labelled Comp Radiopharm.* 2016;59(10):424–428.
20. Chicheportiche A, Marciano R, Orevi M. Comparison of NEMA characterizations for Discovery MI and Discovery MI-DR TOF PET/CT systems at different sites and with other commercial PET/CT systems. *EJNMMI Phys.* 2020;7(1):4.
21. Schneider CA, Rasband WS, Eliceiri KW. NIH Image to ImageJ: 25 years of image analysis. *Nat Methods.* 2012;9(7):671–675.
22. Silver DA, Pellicer I, Fair WR, Heston WD, Cordon-Cardo C. Prostate-specific membrane antigen expression in normal and malignant human tissues. *Clin Cancer Res.* 1997;3(1):81–85.
23. Chang SS, O'Keefe DS, Bacich DJ, Reuter VE, Heston WD, Gaudin PB. Prostate-specific membrane antigen is produced in tumor-associated neovasculature. *Clin Cancer Res.* 1999;5(10):2674–2681.
24. Mahzouni P, Shavakhi M. Prostate-specific membrane antigen expression in neovasculature of glioblastoma multiforme. *Adv Biomed Res.* 2019;8:18.
25. Kunikowska J, Bartosz K, Leszek K. Glioblastoma multiforme: another potential application for 68Ga-PSMA PET/CT as a guide for targeted therapy. *Eur J Nucl Med Mol Imaging.* 2018;45(5):886–887.